

2012

# Structure- and ligand-based drug design approaches for neglected tropical diseases

PURE AND APPLIED CHEMISTRY, RES TRIANGLE PK, v. 84, n. 9, supl. 1, Part 2, pp. 1857-1866, 40544, 2012

http://www.producao.usp.br/handle/BDPI/41675

*Pure Appl. Chem.*, Vol. 84, No. 9, pp. 1857–1866, 2012.
http://dx.doi.org/10.1351/PAC-CON-11-11-07


# Structure- and ligand-based drug design approaches for neglected tropical diseases*

Rafael V. C. Guido, Glaucius Oliva, and Adriano D. Andricopulo‡

*Laboratório de Química Medicinal e Computacional, Instituto de Física de São Carlos, Universidade de São Paulo, Av. Trabalhador São-Carlense 400, 13560-970 São Carlos-SP, Brazil*

*Abstract*: Drug discovery has moved toward more rational strategies based on our increasing understanding of the fundamental principles of protein–ligand interactions. Structure- (SBDD) and ligand-based drug design (LBDD) approaches bring together the most powerful concepts in modern chemistry and biology, linking medicinal chemistry with structural biology. The definition and assessment of both chemical and biological space have revitalized the importance of exploring the intrinsic complementary nature of experimental and computational methods in drug design. Major challenges in this field include the identification of promising hits and the development of high-quality leads for further development into clinical candidates. It becomes particularly important in the case of neglected tropical diseases (NTDs) that affect disproportionately poor people living in rural and remote regions worldwide, and for which there is an insufficient number of new chemical entities being evaluated owing to the lack of innovation and R&D investment by the pharmaceutical industry. This perspective paper outlines the utility and applications of SBDD and LBDD approaches for the identification and design of new small-molecule agents for NTDs.

*Keywords*: biological activity; computer-aided molecular design; drug discovery; enzymes; enzyme inhibitors; ligand-based drug design; medicinal chemistry; neglected tropical diseases; structure-based drug design; structure–activity relationships.

## INTRODUCTION

Neglected tropical diseases (NTDs) place a heavy burden on society in terms of long-term disability, illness, and death, with severe social and economic consequences for millions of people worldwide [1–3]. Despite their high prevalence, in most cases the treatment for NTDs is inadequate and incredibly limited (it is usually characterized by a low efficacy and considerable toxicity of the existing drugs), leading to an urgent and immediate demand for new drugs. However, in addition to the traditional challenges involved in the complex process of drug discovery and development, it is widely recognized that there is an innovation gap and a lack of pharmaceutical R&D investment in the area of NTDs [4–6].

Drug discovery is driven by innovation employing a combination of experimental and computational methods. In this context, the integration of modern drug discovery approaches allowing hit identification and lead optimization, as well as the discovery of innovative new chemical entities, are major challenges in this field [7–11]. The use of structure- (SBDD) and ligand-based drug design (LBDD)

**Pure Appl. Chem.* **84**, 1837–1937 (2012). A collection of invited papers based on presentations on the Chemistry of Life theme at the 43rd IUPAC Congress, San Juan, Puerto Rico, 30 July–7 August 2011.
‡Corresponding author: Tel.: +55 16 3373 8095; Fax: +55 16 3373 9881; E-mail: aandrico@ifsc.usp.br

methods is especially attractive for drug discovery for NTDs [3,12]. Over the past years, SBDD and LBDD have evolved and transformed these approaches in tools of large impact in modern drug design. In general, one of the most important issues that must be addressed during the selection of the appropriate approach is the evaluation of the nature and level of the molecular information available. For instance, LBDD approaches are powerful methods based on only small-molecule information using a series of known active and inactive compounds, whereas SBDD approaches incorporate information from the target receptor [13,14]. It is worth noting that these knowledge-driven approaches can be explored in combination, creating new opportunities for innovation in medicinal chemistry in order to maximize the accomplishment of drug discovery projects. Recent successful examples highlight the diversity of SBDD and LBDD strategies, assembling the most powerful concepts in chemistry and biology, with particular emphasis on the field of NTDs [2,7–9].

This paper outlines the fundamental principles and state of the art in the integration of SBDD and LBDD strategies for the discovery of innovative chemotherapy agents for a variety of NTDs, highlighting advances, limitations, and future perspectives in medicinal chemistry.

## SBDD AND LBDD APPROACHES FOR NEGLECTED TROPICAL DISEASES

A useful strategy for the design of new active compounds against NTDs relies on the investigation of unique biochemical pathways and proteins of the pathogens. In line with this, trypanothione reductase (TR), an essential enzyme of the thiol metabolism in trypanosomatids, has been explored as a molecular target for the development of new chemotherapy agents [15]. TR is a key enzyme of the parasite redox system involved in the protection against oxidative damage and supply of reducing equivalents for DNA synthesis [14,15]. SBDD approaches applied for the development of TR inhibitors have proven challenging owing to the difficulty of determining the binding modes of several ligands. Nonetheless, molecular modeling strategies have been employed to provide useful structural information for inhibitor drug design [16–18]. An important example is the design of a series of diaryl sulfide-based derivatives as new TR inhibitors [19]. In this work, molecular docking strategies were employed for the previously reported lead compound BTCP ($K_i$ = 1 μM) [18], suggesting the binding of the ligand to the hydrophobic Z-site of the TR enzyme (Fig. 1A). Exploring the integration of SBDD (e.g., molecular docking) and LBDD (e.g., energy minimization and conformational analysis) approaches, a diaryl sulfide analog (TR inhibition = 36 %, at 100 μM) containing a central imidazole moiety was predicted to simultaneously bind to the mepacrine binding site and the hydrophobic patch of the TR catalytic cavity (Fig. 1B). According to the model, the presence of bulky substituents on the piperazine moiety could positively influence the inhibitory activity of new derivatives through the occupation of the hydrophobic Z-site. In addition, a combination of the imidazole-based diaryl sulfide derivative with BTCP would optimize the interactions with the TR binding pocket, and therefore yield a compound with higher binding affinity (Fig. 1C). Following this, 48 triazole- and imidazole-based diaryl sulfide derivatives were synthesized and evaluated against TR. The results showed that seven derivatives exhibited significant TR inhibition (TR inhibition > 50 %, at 40 μM). As expected, the most promising inhibitor (**1**) ($K_i$ = 0.51 μM, Fig. 1D) showed a competitive type of inhibition with respect to the substrate trypanothione disulfide ($TS_2$), and at the concentration of 20 μM, did not affect the activity of the human homolog glutathione reductase (GR, 40 % sequence identity to TR) [19]. Additionally, compound **1** exhibited in vitro activity in the sub- to low micromolar range against a panel of protozoan parasites, including *Trypanosoma cruzi*, *Trypanosoma brucei rhodesiense*, *Leishmania donovani*, and *Plasmodium falciparum*, with selectivity index (SI) between 4 and 165 (SI = $IC_{50}$ L6 cells/$IC_{50}$ parasite).

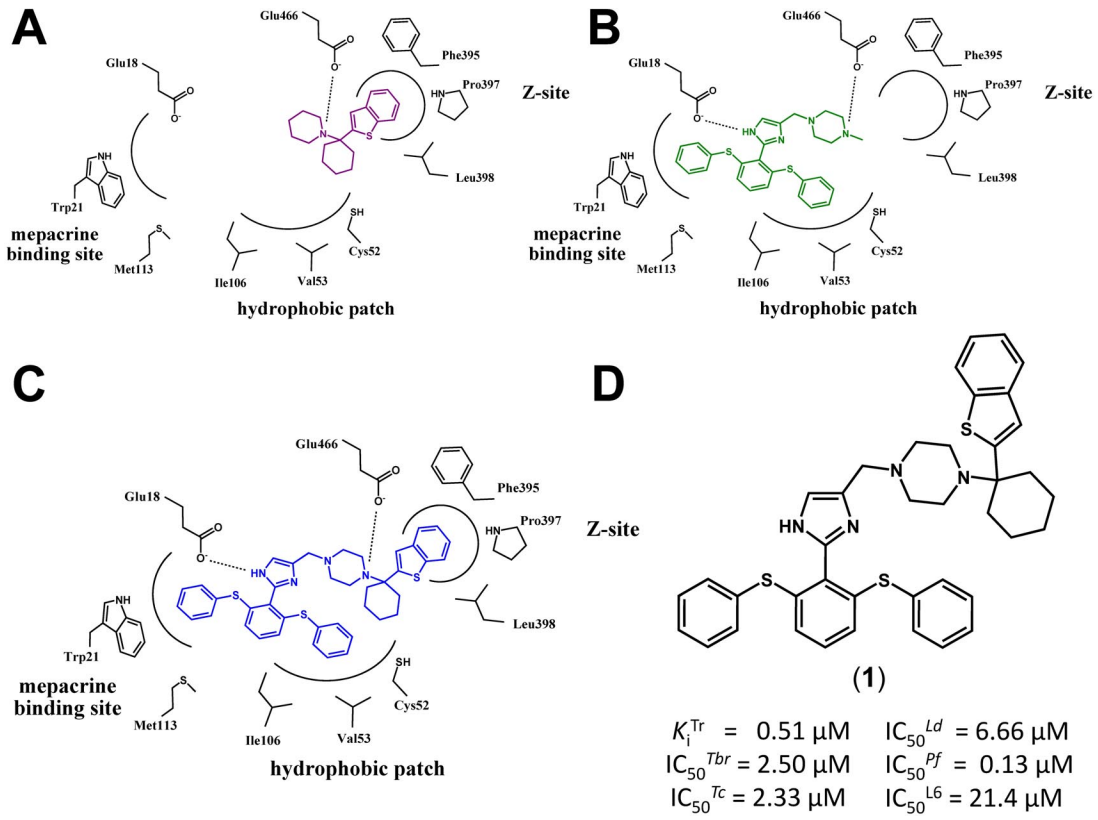


**Fig. 1** Predicted binding mode of BCTP (**A**), imidazole-based diaryl sulfide derivative (**B**) and conjugated compound (**1**) (**C**). Biological data for compound (**1**) (**D**) (Tr = trypanothione reductase enzyme; *Tbr* = *T. brucei rhodesiense*; *Tc* = *T. cruzi*; *Ld* = *L. donovani*; *Pf* = *P. falciparum*; L6 = rat myoblast L6 cells line strains to assess cytotoxicity).

Detailed structural information of several parasite enzymes is available in public databases such as the Protein Data Bank (PDB) [20]. The combination of structural data and chemogenomics approaches is useful for the evaluation of the biological relevance and "druggability" profile (i.e., the likelihood that a target is amenable to functional modulation through interaction with a therapeutic agent) of these target proteins [21–23]. The strategy highlights attractive molecular targets for SBDD, providing new opportunities for hit identification and lead discovery [12]. In this context, organisms such as *T. brucei*, *T. cruzi*, and *P. falciparum* have several key enzymes implicated in pathogenesis and host cell invasion, including a number of closely related proteases [24,25]. In *P. falciparum*, plasmepsins (aspartic protesases) and falcipains (cysteine proteases) catalyze the degradation of host hemoglobin to provide nutrients for exponential growth and maturation of the pathogen [26]. Indeed, the cysteine proteases falcipain-2, -2', and -3 play an important role in *Plasmodium* development, and their inhibition may suppress parasite growth [27]. Similarly, in trypanosomatids, the cysteine proteases rhodesain (cathepsin L-like) and cathepsin B (*Tb*CatB, cathepsin B-like) from *T. brucei* and cruzain (cathepsin L-like) from *T. cruzi* play a pivotal role during the infection of host cells, replication, and metabolism [24]. Overall, this class of enzymes is among the most investigated targets for the development of new antitrypanosomal agents. The protozoan enzymes falcipain, rhodesain, *Tb*CatB, and cruzain share common features of the cysteine proteases family, such as the classical papain fold consisting of two distinct domains (Fig. 2A). The superimposition of the structures reveals a high degree of structural similarity (Cα RMSD: 0.5–2.5 Å), with the highest conservation observed in the catalytic

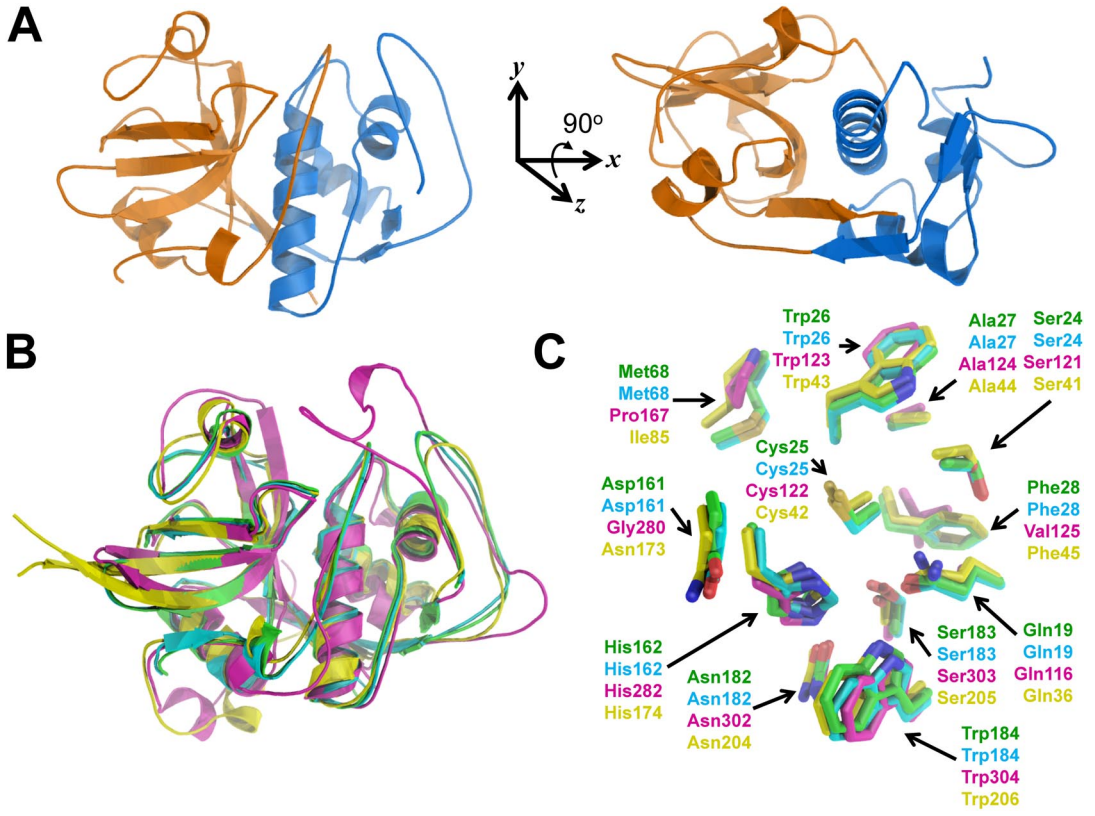


**Fig. 2** (**A**) Papain cysteine protease family representative fold consisting of two distinct domains. (**B**) Superimposition of the X-ray crystal structures of rhodesain (green, PDB ID: 2P86), cruzain (cyan, PDB ID: 3I06) *Tb*catB (magenta, PDB ID: 3HHI) and falcipain-2 (yellow, PDB ID: 3BPF). (**C**) Superimposition of the key amino acid residues in the catalytic site of rhodesain (green), cruzain (cyan), *Tb*catB (magenta), and falcipain-2 (yellow).

domain (Cα RMSD: 0.3–0.4 Å). The catalytic dyad (cruzain = Cys25 and His 162; rhodesain = Cys25 and His 162; *Tb*catB = Cys 122 and His 282; falcipain = Cys 42 and His 174) is embedded in a channel-like junction between the two domains with highly conserved amino acids (Fig. 2B). Therefore, cysteine protease inhibitors could be useful lead candidates for these related parasitic infections.

In general, cysteine protease inhibitors exhibit an electrophilic functional group to form an irreversible or reversible covalent thioimidate intermediate with the catalytic cysteine [28]. In line with this, a series of triazine nitrile derivatives was designed as potent inhibitors of rhodesain and falcipain-2 [29]. Molecular modeling studies provided useful insights into the binding mode and structure–activity relationship (SAR) of this series of inhibitors. The results highlighted the importance of the diamino-substituted triazine core structure to direct the orientation of substituents in the S1, S2, and S3 binding pockets. The predicted binding mode of the lead compound (**2**) suggests key features, including (i) a morpholine group as substituent to occupy the S1 pocket, (ii) a 4-(n-propyl)cyclohexyl substituent to occupy the hydrophobic S2 pocket, and (iii) a 1,3-benzodioxol-5-yl moiety to interact with the S3 pocket (Fig. 3A). Thus, a series of 17 triazine nitrile derivatives was synthesized and evaluated against rhodesain and falcipain-2. The most promising competitive inhibitor (**3**) showed inhibitory potency in the low nanomolar range (Fig. 3B). Compound (**3**) showed no inhibition against a panel of proteases, including human cathepsin B, viral cysteine proteases as well as α-chymotrypsin (serine protease). In

 

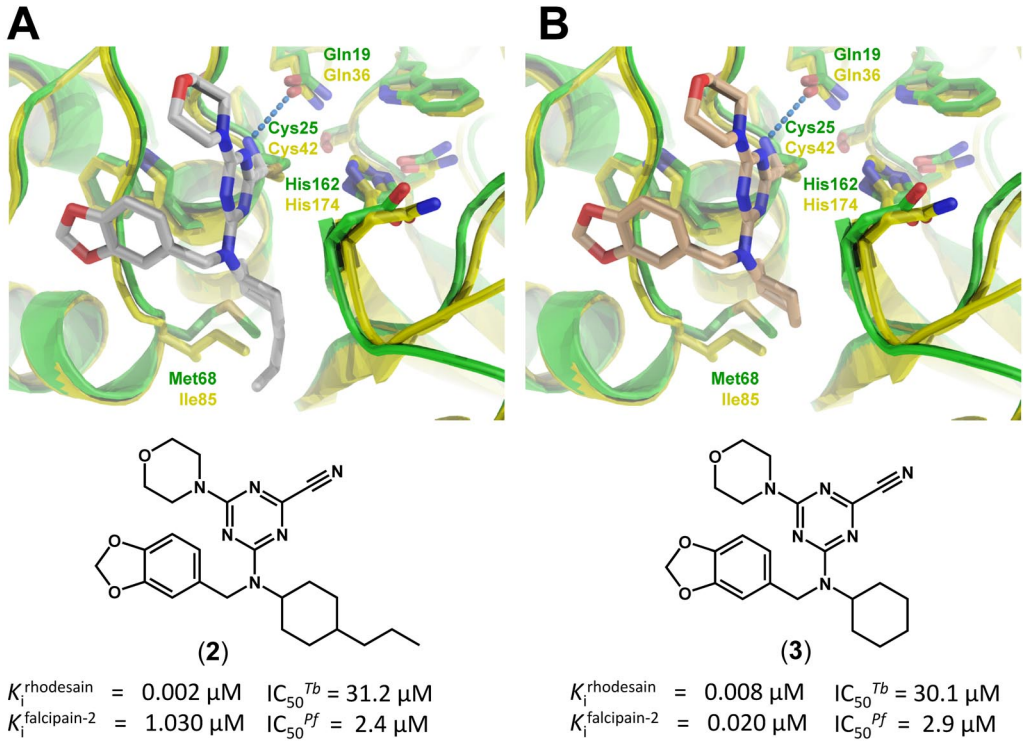


**Fig. 3** Molecular structure, biological data, and predicted binding mode of the lead compound (**2**) (**A**), and the most promising cysteine protease inhibitor (**3**) (**B**) into the binding pocket of rhodesain (green) and falcipain-2 (yellow). Hydrogen bonds are depicted as blue dashed lines (*Tb* = *Trypanosoma brucei rhodesiense*; *Pf* = *Plasmodium falciparum*).

addition, compound **3** exhibited moderate in vitro growth inhibitory activity against *T. brucei rhodesiense* ($IC_{50}$ = 30.1 µM) and *P. falciparum* ($IC_{50}$ = 2.9 µM).

In the past decade, the development of a number of irreversible inhibitors of cruzain has demonstrated the usefulness of this approach in inhibitor drug design for infectious diseases [30]. In order to identify new reversible covalent inhibitors of cruzain, high-throughput screening (HTS) was conducted employing approximately 200 000 compounds from the NIH Molecular Library [31]. The identification of reversible inhibitors offers the potential of fewer off-target binding and side-effects, which are frequently associated with irreversible enzyme inhibitors. The screening hits prioritized belong to several classes of molecular scaffolds. The counter screening process on these promising chemotypes confirmed the triazine derivative (**4**) as an inhibitor of cruzain, with a $K_i$ value of 180 nM (Fig. 4A). Further kinetic investigations revealed a reversible and competitive type of inhibition. Hit-to-lead and SAR studies indicated that hydrophobic substituents at the 4-amino group, electron-withdrawing substituents at the 6-phenylamino group, as well as structural rigidity were favorable for cruzain inhibition. The latter observation was accomplished by the generation of purine-derived nitriles as new lead compounds. The incorporation of these features led to compound **5**, which exhibited potent inhibition of the target enzyme with an $IC_{50}$ of 0.2 nM (Fig. 4B). These results encouraged the development of X-ray crystallography studies, and the high-resolution complex obtained (1.1 Å) not only revealed important molecular aspects responsible for the biological activity of this series of inhibitors, but also indicated relevant structural elements involved in the covalent, reversible inhibition mechanism (Fig. 4C). For instance, the formally linear nitrile became a planar imino-moiety as the covalent adduct with the catalytic Cys25 is formed. Additionally, the purine moiety binds between the S1 and S2 pockets, the aromatic ring at

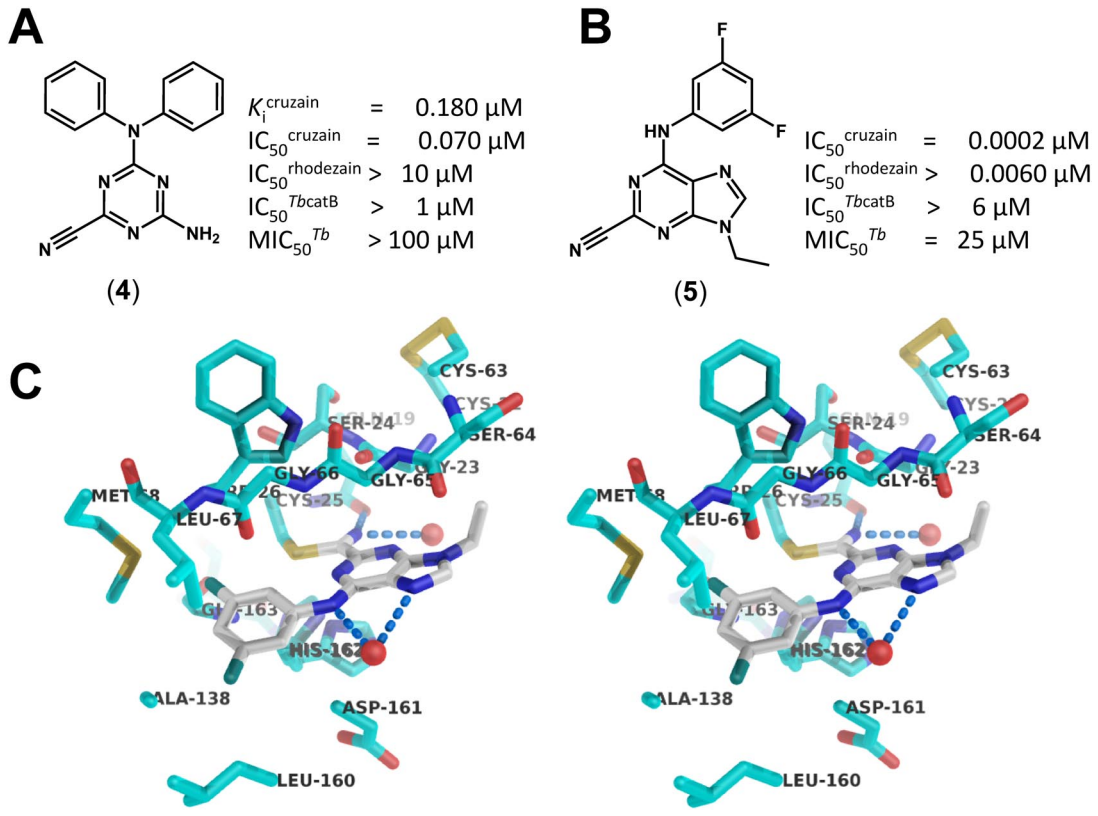


**Fig. 4** Molecular structure and biological data of the HTS hit (**4**) (**A**), and of the developed compound (**5**) (**B**) (*Tb* = *Trypanosoma brucei*). (**C**) Experimental binding mode of the compound (**5**) within the cruzain catalytic site (PDB ID: 3I06). Hydrogen bonds are depicted as blue dashed lines, and crystallographic water molecules as red spheres.

the *N*6-position extends into the hydrophobic S2 pocket and the *N*9-ethyl substituent is solvent-exposed, suggesting an attractive position for the improvement of pharmacokinetic properties (Fig. 4C). Considering the structural similarities of the parasite's cysteine proteases, compound **5** was also evaluated against the *T. brucei* homologs rhodesain and *Tb*catB, showing inhibitory potency in the low namolar ($IC_{50}$ = 60 nM) and micromolar ($IC_{50}$ = 6 μM) ranges, respectively (Fig. 4B). In spite of its cruzain inhibitory activity, compound **5** was not active against whole cell cultures of *T. cruzi*. Conversely, promising activity was detected against *T. brucei* ($MIC_{50}$ = 25 μM, Fig. 4B). The selectivity profile of **5** was evaluated over a panel of 71 proteases, including 22 cysteine proteases, 4 aspartyl proteases, 26 serine proteases, 5 peptidases, and 14 matrix metalloproteinases. Compound **5** was active only against closely related cysteine proteases, however, with significant SI values ranging from 80 (cathepsin-S) to 50.000 (cathepsin-B).

The integration of SBDD and LBDD approaches has found its way into drug discovery programs for NTDs [32–38]. Good examples can be seen in the use of 3D QSAR methods, such as comparative molecular field analysis (CoMFA) [39,40] and comparative molecular similarity index analysis (CoMSIA) [41,42]. These QSAR methods rely on the relative spatial orientation of series of ligands (structural alignment) into the binding site of the target protein. The 3D structure of the protein along with an appropriate docking tool is used to guide the molecular alignment of the dataset for the QSAR analysis. The quality of the conformations of the compounds (superposition of the bioactive molecules) is of fundamental importance for all subsequent procedures. The combined approach, which incorpo-

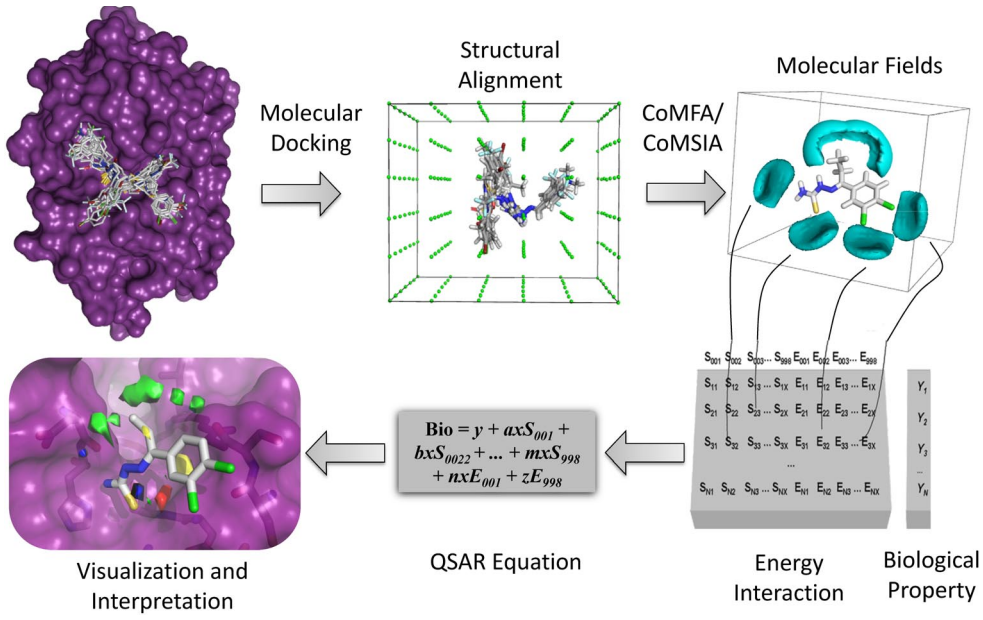


**Fig. 5** Integration of SBDD and LBDD with 3D QSAR methods.

rates components at the micro- and macromolecular level, allows the generation of a target-specific scoring method considering the available chemical and biological data (Fig. 5).

A number of successful examples of the application of this drug design strategy have been reported in the area of NTDs [43–46]. For instance, CoMFA and CoMSIA methods were employed to investigate a large series of adenosine analogs, exploring structural differences between the human and trypanosomatid glyceraldehyde-3-phosphate dehydrogenase (GAPDH) enzymes [47]. The integration of molecular docking and 3D QSAR was a useful strategy for the generation of highly predictive models. In addition, the CoMFA and CoMSIA contour maps, representing the effects of the steric, electrostatic, hydrophobic, and hydrogen-bond donor and acceptor molecular fields, allowed the identification of key chemical and structural features responsible for selectivity and biological potency [47]. Similarly, molecular modeling studies were carried out in order to identify the preferred binding mode of a series of thiosemicarbazone derivatives as covalent reversible inhibitors of cruzain [48]. Docking investigations led to the identification of the essential structural requirements for the molecular alignment, and robust CoMFA and CoMSIA models were developed on the basis of the predicted bioactive conformations. The models possessed high internal and external consistency, showing substantial predictive power. Additionally, detailed analysis of the CoMFA electrostatic maps provided structural insights into the reversible covalent mechanism of inhibition of this class of compounds. According to the model, key hydrogen bond interactions may play an important role in the backward reaction [48].

Several steps of the drug discovery process (e.g., hit identification, lead optimization, NCE discovery) can be improved in a rational way with the application of SBDD and LBDD methods [2,7–9]. In this context, virtual screening has become a highly valued and widely used tool for the identification of hits and lead compounds for a variety of therapeutically important target proteins [2,49–52]. An example can be seen in the medicinal chemistry approach employed for the discovery of new inhibitors of *Schistosoma mansoni* purine nucleoside phosphorylase (*Sm*PNP), which outlines a successful scenario for the integration of computational and experimental methods. PNP is a key enzyme involved in the purine salvage pathway of *S. mansoni*, one of the causative agents of human schistosomiasis [53,54]. In this work, a structure-based pharmacophore model was employed for the virtual screening of a huge library of compounds, leading to the identification of three thioxothiazolidinones derivatives

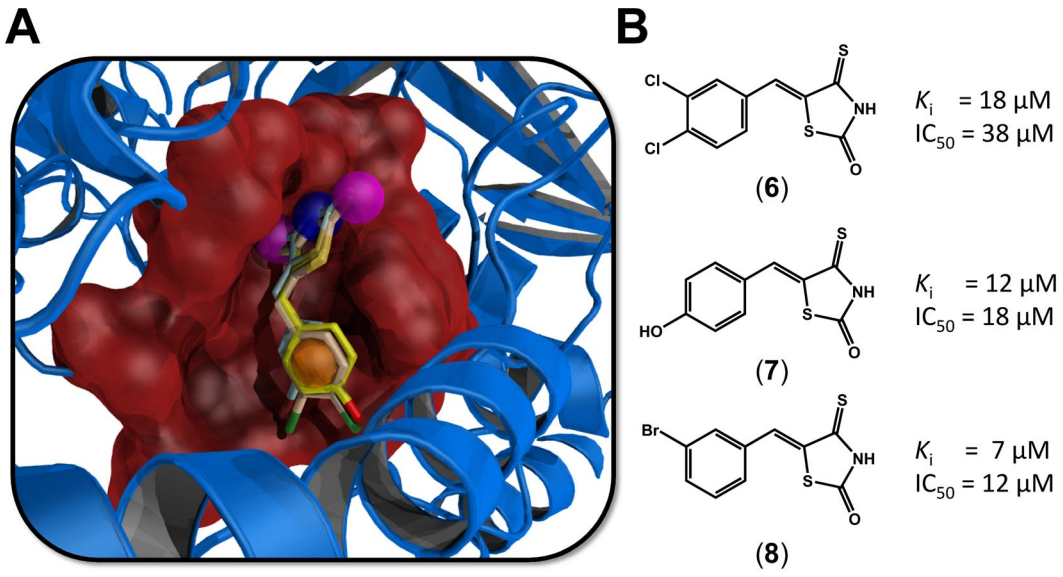


**Fig. 6** (**A**) Predicted binding mode of the lead compounds (**6**) (beige), (**7**) (yellow), and (**8**) (light blue) overlaid on the four-point structure-based pharmacophore model employed in the virtual screening of a large database of commercially available compounds. The hydrophobic favorable region within the *Sm*PNP binding site is indicated as an orange sphere; donor and acceptor favorable regions are depicted as blue and magenta spheres, respectively. (**B**) Molecular structure and biochemical data of the reversible and competitive *Sm*PNP inhibitors.

with substantial in vitro inhibitory activity against *Sm*PNP (Fig. 6A) [55]. Convenient synthesis, biochemical evaluation, and SAR studies led to the successful development of a set of thioxothiazolidinone derivatives harboring a novel chemical scaffold as new competitive inhibitors of *Sm*PNP in the low micromolar range. The most potent inhibitors (**6–8**) represent new lead compounds for further development for the therapy of schistosomiasis (Fig. 6B).

## CONCLUSIONS

In the past years, SBDD and LBDD have been successfully applied in the identification and development of several new classes of inhibitors of key enzymes for NTDs. The integration of these approaches is a useful and valuable tool for the prioritization of compounds for further investigation involving computational and experimental methods. In spite of the intrinsic technical limitations, there are many examples demonstrating the cost effectiveness and reliability of these methods in the generation of lead compounds. Noteworthy, the structural diversity of the compounds identified considerably differs from the drugs currently available, thereby providing good starting points for lead optimization, as well as for the discovery of high-quality new chemical entities. Although there are many fundamental aspects to be further explored in the integration of SBDD and LBDD, these approaches will continue to evolve and have considerable impact in the development of new drug candidates for parasitic diseases, and it is likely to remain as such for the foreseeable future.

## ACKNOWLEDGMENTS

We gratefully acknowledge financial support from the State of São Paulo Research Foundation (FAPESP) and from the National Council for Scientific and Technological Development (CNPq), Brazil.

 

## REFERENCES


1. P. G. Ruminski. *Future Med. Chem.* **3**, 1253 (2011).
2. R. S. Ferreira, R. V. C. Guido, A. D. Andricopulo, G. Oliva. *Expert Opin. Drug Discov.* **6**, 481 (2011).
3. E. Chatelain, J. R. Ioset. *Drug Discov. Dev. Ther.* **5**, 175 (2011).
4. J. Cohen, M. S. Dibner, A. Wilson. *PLoS One* **5**, e10610 (2010).
5. P. H. Jakobsen, M. W. Wang, S. Nwaka. *PLoS Negl. Trop. Dis.* **5**, e1221 (2011).
6. S. Nwaka, B. Ramirez, R. Brun, L. Maes, F. Douglas, R. Ridley. *PLoS Negl. Trop. Dis.* **3**, e440 (2009).
7. L. D. Chiaradia, P. G. A. Martins, M. N. S. Cordeiro, R. V. C. Guido, G. Ecco, A. D. Andricopulo, R. A. Yunes, J. Vernal, R. J. Nunes, H. Terenzi. *J. Med. Chem.* **55**, 390 (2012).
8. A. D. Andricopulo, R. A. Yunes, R. J. Nunes, A. O. S. Savi, R. Correa, A. B. Cruz, V. Cechinel. *Quim. Nova* **21**, 573 (1998).
9. R. V. C. Guido, G. Oliva, A. D. Andricopulo. *Comb. Chem. High Throughput Screening* **14**, 830 (2011).
10. L. Tan, J. Batista, J. Bajorath. *Chem. Biol. Drug Des*. **76**, 191 (2010).
11. T. T. Talele, S. A. Khedkar, A. C. Rigby. *Curr. Top. Med. Chem.* **10**, 127 (2010).
12. R. V. C. Guido, G. Oliva. *Curr. Top. Med. Chem.* **9**, 824 (2009).
13. P. J. Hajduk, J. Greer. *Nat. Rev. Drug Discov.* **6**, 211 (2007).
14. L. B. Salum, A. D. Andricopulo. *Mol. Divers.* **13**, 277 (2009).
15. V. Olin-Sandoval, R. Moreno-Sanchez, E. Saavedra. *Curr. Drug Targets* **11**, 1614 (2010).
16. R. L. Krauth-Siegel, H. Bauer, H. Schirmer. *Angew. Chem., Int. Ed.* **44**, 690 (2005).
17. R. L. Krauth-Siegel, O. Inhoff. *Parasitol. Res.* **90**, S77 (2003).
18. S. Patterson, D. C. Jones, E. J. Shanks, J. A. Frearson, I. H. Gilbert, P. G. Wyatt, A. H. Fairlamb. *ChemMedChem* **4**, 1341 (2009).
19. C. Eberle, B. S. Lauber, D. Fankhauser, M. Kaiser, R. Brun, R. L. Krauth-Siegel, F. Diederich. *ChemMedChem* **6**, 292 (2011).
20. H. M. Berman, J. Westbrook, Z. Feng, G. Gilliland, T. N. Bhat, H. Weissig, I. N. Shindyalov, P. E. Bourne. *Nucleic Acids Res.* **28**, 235 (2000).
21. M. Bredel, E. Jacoby. *Nat. Rev. Genet.* **5**, 262 (2004).
22. C. J. Harris, A. P. Stevens. *Drug Discov. Today* **11**, 880 (2006).
23. Y. L. Yang, S. J. Adelstein, A. I. Kassis. *Drug Discov. Today* **14**, 147 (2009).
24. J. H. McKerrow, P. J. Rosenthal, R. Swenerton, P. Doyle. *Curr. Opin. Infect. Dis.* **21**, 668 (2008).
25. J. H. McKerrow, C. Caffrey, B. Kelly, P. Loke, M. Sajid. *Annu. Rev. Pathol.* **1**, 497 (2006).
26. L. H. Miller, D. I. Baruch, K. Marsh, O. K. Doumbo. *Nature* **415**, 673 (2002).
27. C. Teixeira, J. R. B. Gomes, P. Gomes. *Curr. Med. Chem.* **18**, 1555 (2011).
28. J. H. McKerrow, J. C. Engel, C. R. Caffrey. *Bioorg. Med. Chem.* **7**, 639 (1999).
29. V. Ehmke, C. Heindl, M. Rottmann, C. Freymond, W. B. Schweizer, R. Brun, A. Stich, T. Schirmeister, F. Diederich. *ChemMedChem* **6**, 273 (2011).
30. K. Brak, P. S. Doyle, J. H. McKerrow, J. A. Ellman. *J. Am. Chem. Soc.* **130**, 6404 (2008).
31. B. T. Mott, R. S. Ferreira, A. Simeonov, A. Jadhav, K. K. H. Ang, W. Leister, M. Shen, J. T. Silveira, P. S. Doyle, M. R. Arkin, J. H. McKerrow, J. Inglese, C. P. Austin, C. J. Thomas, B. K. Shoichet, D. J. Maloney. *J. Med. Chem*. **53**, 52 (2010).
32. R. V. C. Guido, G. H. Trossini, M. S. Castilho, G. Oliva, E. I. Ferreira, A. D. Andricopulo. *J. Enzyme Inhib. Med. Chem.* **23**, 964 (2008).
33. K. M. Honorio, R. C. Garratt, I. Polikarpov, A. D. Andricopulo. *J. Mol. Graphics Model.* **25**, 921 (2007).
34. R. V. C. Guido, M. S. Castilho, S. G. R. Mota, G. Oliva, A. D. Andricopulo. *QSAR Comb. Sci.* **27**, 768 (2008).


 

35. C. L. Cardoso, V. V. Lima, A. Zottis, G. Oliva, A. D. Andricopulo, I. W. Wainer, R. Moaddel, Q. B. Cass. *J. Chromatogr., A* **1120**, 151 (2006).
36. R. V. C. Guido, C. L. Cardoso, M. C. de Moraes, A. D. Andricopulo, Q. B. Cass, G. Oliva. *J. Braz. Chem. Soc.* **21**, 1845 (2010).
37. K. N. de Oliveira, L. D. Chiaradia, P. G. A. Martins, A. Mascarello, M. N. S. Cordeiro, R. V. C. Guido, A. D. Andricopulo, R. A. Yunes, R. J. Nunes, J. Vernal, H. Terenzi. *MedChemComm* **2**, 500 (2011).
38. A. Mascarello, L. D. Chiaradia, J. Vernal, A. Villarino, R. V. Guido, P. Perizzolo, V. Poirier, D. Wong, P. G. Martins, R. J. Nunes, R. A. Yunes, A. D. Andricopulo, Y. Av-Gay, H. Terenzi. *Bioorg. Med. Chem.* **18**, 3783 (2010).
39. R. D. Cramer, D. E. Patterson, J. D. Bunce. *J. Am. Chem. Soc.* **110**, 5959 (1988).
40. R. D. Cramer 3rd, D. E. Patterson, J. D. Bunce. *Prog. Clin. Biol. Res.* **291**, 161 (1989).
41. G. Klebe, U. Abraham, T. Mietzner. *J. Med. Chem.* **37**, 4130 (1994).
42. G. Klebe, U. Abraham. *J. Comput.-Aided Mol. Des.* **13**, 1 (1999).
43. I. Garcia, Y. Fall, G. Gomez. *Curr. Pharm. Des.* **16**, 2666 (2010).
44. I. Garcia, Y. Fall, G. Gomez. *Curr. Bioinf.* **6**, 215 (2011).
45. K. K. Roy, S. S. Bhunia, A. K. Saxena. *Chem. Biol. Drug Des.* **78**, 483 (2011).
46. A. H. Xie, S. Odde, S. Prasanna, R. J. Doerksen. *J. Comput.-Aided Mol. Des.* **23**, 431 (2009).
47. R. V. C. Guido, G. Oliva, C. A. Montanari, A. D. Andricopulo. *J. Chem. Inf. Model.* **48**, 918 (2008).
48. G. H. Trossini, R. V. Guido, G. Oliva, E. I. Ferreira, A. D. Andricopulo. *J. Mol. Graph. Model.* **28**, 3 (2009).
49. P. B. McKay, M. B. Peters, G. Carta, C. T. Flood, E. Dempsey, A. Bell, C. Berry, D. G. Lloyd, D. Fayne. *Bioorg. Med. Chem. Lett.* **21**, 3335 (2011).
50. G. F. Ruda, G. Campbell, V. P. Alibu, M. P. Barrett, R. Brenk, I. H. Gilbert. *Bioorg. Med. Chem.* **18**, 5056 (2010).
51. M. Jacobsson, M. Garedal, J. Schultz, A. Karlen. *J. Med. Chem.* **51**, 2777 (2008).
52. P. V. Desai, A. Patny, J. Gut, P. J. Rosenthal, B. Tekwani, A. Srivastava, M. Avery. *J. Med. Chem.* **49**, 1576 (2006).
53. M. S. Castilho, M. P. Postigo, H. M. Pereira, G. Oliva, A. D. Andricopulo. *Bioorg. Med. Chem.* **18**, 1421 (2010).
54. M. P. Postigo, R. Krogh, M. F. Terni, H. M. Pereira, G. Oliva, M. S. Castilho, A. D. Andricopulo. *J. Braz. Chem. Soc.* **22**, 583 (2011).
55. M. P. Postigo, R. V. Guido, G. Oliva, M. S. Castilho, R. P. I. da, J. F. de Albuquerque, A. D. Andricopulo. *J. Chem. Inf. Model.* **50**, 1693 (2010).

 